Acta Polytechnica CTU Proceedings **53**:42–48, 2025
https://doi.org/10.14311/APP.2025.53.0042

Published by the Czech Technical University in Prague

PARAMETRIC STUDY OF A REINFORCED CONCRETE FOOTBRIDGE STRENGTHENED BY A LAYER OF UHPFRC

Petr Kněž, Milan Holý*, Jiří Kolísko

Czech Technical University in Prague, Klokner Institute, Šolínova 7, Prague 166 08, Czech Republic

* corresponding author: Milan.Holy@cvut.cz

Abstract. This paper deals with the presentation of a parametric study of the strengthening of a reinforced concrete footbridge with a layer of reinforced UHPFRC on its upper surface. In order to increase its load carrying capacity, stiffness and durability, the design of strengthening with 50 mm thick UHPFRC layer was carried out. The geometry of the analyzed structure is based on the real structure. The parametric study solves its strengthening by considering different support options of the structure and its degradation. The design and assessment was carried out in the form of nonlinear numerical analysis using the FEM in Atena 3D.

Keywords: UHPFRC, footbridge, reinforced concrete, strengthening, degradation, FEA.

1. Introduction

The parametric study of the effect of strengthening [1–6] the reinforced concrete structure with a UHPFRC [7] layer was based on an existing reinforced concrete footbridge. The existing footbridge is located in the tank of a chemical plant and shows structural damage after years of operation. The footbridge is used to access the platform, which is located in the centre of the chemical tank on 4 circular columns. The footbridge is supported at one end by a central platform and at the other end by the tank wall. Both supports are considered to be fixed. For the parametric study, two other methods of supporting the footbridge were considered. The first considered a fixed support at the location of the central platform and an hinged support at the tank wall. The second method of support considered a hinge at each end of the footbridge. The structure is symmetrical, see Figure 1.

The parametric study was focused on the evaluation of the influence of the 50 mm thick reinforced UHPFRC layer on the upper surface of the reinforced concrete structure. The load bearing capacity as a function of the degradation of the original structure and the boundary support conditions was investigated. The load bearing capacity of the strengthened structure was compared with the load bearing capacity of reinforced concrete structure without degradation. The study was carried out using nonlinear FEA [8–10] in Atena 3D software.

The footbridge has a length of 8.28 m and a rectangular cross-section with a width of 1.2 m and a height of 0.6 m. One end of the footbridge is embedded in a central reinforced concrete platform. The footbridge is reinforced at both surfaces with 6 ⌀22 mm bars, which are supplemented by ⌀8 mm stirrups at a distance of 400 mm. There is a 50 mm layer of concrete on the footbridge, which serves as a footing and protective layer for the structure. This layer will be replaced by a UHPFRC layer to strengthen the structure. The footbridge is made of C16/20 class concrete and the reinforcing bars are made of 10 216 (E) class steel. The design of the footbridge and its reinforcement is shown in Figure 1. The degradation of the reinforced concrete structure includes a reduction of the modulus of elasticity and strength characteristics of the concrete as well as 15 % reduction of the reinforcement cross-sectional area due to corrosion.

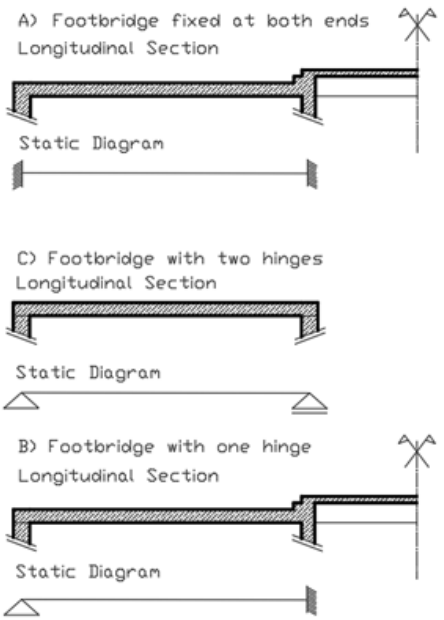

Figure 1. Longitudinal sections and structural diagrams of the considered structural variants of the footbridge.

The new layer made of UHPFRC class C120 FR6 with 2 % steel fibre content is then reinforced with a welded 150/150 mesh made of ⌀6 mm bars in the axis of the slab with a thickness of 50 mm. The coupling to the footbridge slab is carried out by the use of

Material	E [GPa]	ν [-]	f_c [MPa]	f_t [MPa]	ρ [kg m^{-3}]
C16/20 Mean	29	0.2	24	1.9	2 300
C16/20 Degraded	18	0.2	12	1	2 300
C120 FR6	40	0.2	132	6.0	2 600

TABLE 1. Material characteristics for concrete and UHPFRC.

Material	E [GPa]	f_y [MPa]	f_u [MPa]	ϵ_{lim} [-]	ρ [kg m^{-3}]
B500	200	500	578	0.05	7 850
10216 (E)	200	210	500	0.25	7 850

TABLE 2. Material characteristics for concrete and UHPFRC.

⌀8 mm coupling studs in the number of 8 pcs m^{-2} and alternatively with shear notches.

2. Specifications of the parametric study

The basic division of the study is into three groups based on the boundary conditions of the footbridge support. The first group consists of the footbridge fixed at both ends, the second group consists of the footbridge hinged at one end and fixed at the other. The last group consists of a footbridge with hinges at both ends.

For each support option, several design settings are analysed. The load bearing capacity of the structure in the ideal state without strengthening is verified as a reference state. The ideal condition represents a structure without concrete degradation and without reinforcement corrosion. Furthermore, the load bearing capacity of the variously degraded structure without and with strengthening is verified. The degradation of the reinforced concrete footbridge always consists of a reduction in the material properties of the concrete (modulus of elasticity, tensile strength and compressive strength), which is combined with a 15 % reduction of the reinforcement cross-sectional area, which represent reduction due to corrosion. Variants considering a degraded structure are subsequently strengthened with a layer of UHPFRC of thickness 50 mm, which replaces the original concrete layer covering the footbridge surface. The UHPFRC layer is considered with or without full shrinkage. Full shrinkage is an option for monolithic construction, construction without shrinkage is an option for possible prefabrication. Its coupling to the reinforced concrete footbridge is created by using coupling studs and, alternatively, in combination with shear notches. Thus, 5 analyses are performed for each variant of boundary conditions.

3. Numerical analysis

All of the above mentioned variants of the parametric study are analyzed in Atena 3D. This is a program that allows nonlinear FEA, specialised in concrete structures, where it also allows the monitoring of the possible development of cracks. The geometric, material and contact types of nonlinearities are considered in the calculations.

3.1. Materials and material models

For the purpose of the analysis, several materiel types are considered using different material models [11]. The material model "CC3D Cementitious 2" for normal concrete C16/20 is used and "CC3D Cementitious 2 – User" for UHPFRC C120 FR6 with scattered reinforcement is used. The material property values are given in Table 1.

The second group of materials are steel reinforcing bars and coupling studs. The concrete reinforcement is made of steel class 10216 (E), for the coupling studs and reinforcement of the UHPFRC slab, reinforcement of class B500B is considered. For both steel types the material model "CC3D Reinforcement" [11] is used. The values of the material properties are given in Table 2.

3.2. Numerical models

Five models were created in software Atena 3D for each variation of the boundary conditions of the footbridge supports. For the footbridge with hinged support at both ends(Figure 5), the follow-up part of the reinforced concrete platform is not considered in the model.

The following models were created:

A) The first model consisted of a reinforced concrete footbridge with ideal material properties and no corrosion loss of the reinforcement. The dimensions and reinforcement corresponds to that shown in Chapter 1 (Figure 2).

B) The second model differs from the first only in the material characteristics of the concrete used (degraded concrete) and in the consideration of 15 % reduction of the reinforcement cross-sectional area due to corrosion.

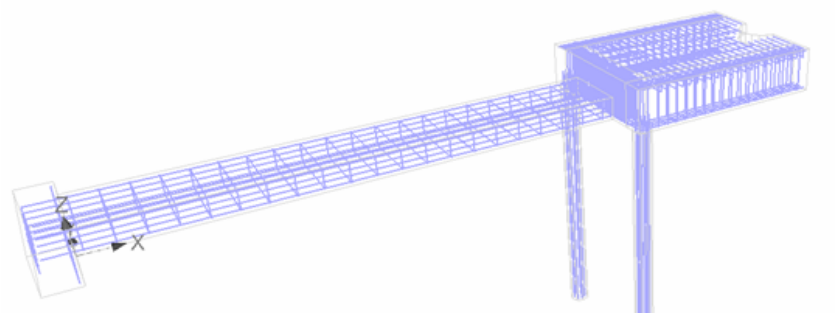

Figure 2. Numerical model of the reinforced concrete footbridge and part of the platform with reinforcement.

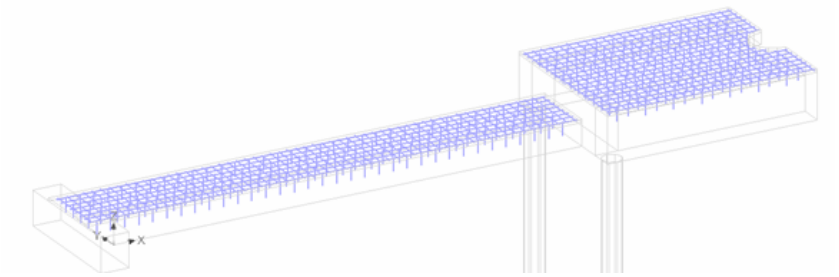

Figure 3. Numerical model with UHPFRC slab, its reinforcement and coupling studs.

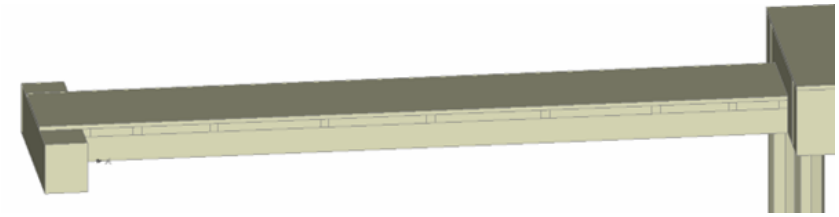

Figure 4. Numerical model of reinforced concrete footbridge connected to a UHPFRC slab by shear notches.

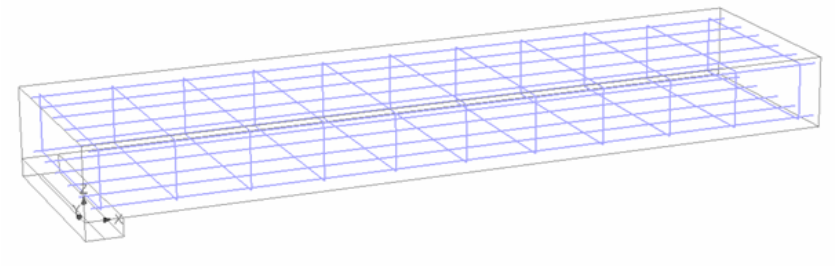

Figure 5. Symmetrical half of the hinge-supported version of the footbridge.

C) The third model is based on the second model, which has been strenghtened with a UHPFRC slab that is coupled to the reinforced concrete structure by using coupling studs. Shrinkage is considered for the UHPFRC slab (Figure 3).

D) The fourth model is identical to the third model, except that shrinkage of the UHPFRC slab is not considered.

E) The fifth model is again a strenghtened degraded reinforced concrete footbridge with a UHPFRC layer, in this case the coupling is created by a combination of shear notches and coupling studs. Shrinkage was not considered for this model (Figure 4).

3.3. Loads

In the calculation, the loads were divided into three types:

- The first type of load was the dead weight of the structure, which is calculated automatically based on the specified volumetric mass of concrete ($2\,400\,\mathrm{kg\,m^{-3}}$), UHPFRC ($2\,600\,\mathrm{kg\,m^{-3}}$) and reinforcing bars ($7\,850\,\mathrm{kg\,m^{-3}}$).
- The second type of load is the remaining dead load. This is only considered for models without a UHPFRC slab where there is a 50 mm layer of concrete on the footbridge – for these models a load of $1.25\,\mathrm{kN\,m^{-2}}$ is considered.
- The third type of load is the service load of the struc-

ture. This is applied in increments of $1\,\mathrm{kN\,m^{-2}}$ until the analysis fails. In addition to the maximum load values before failure, the deformations for a service load of $5\,\mathrm{kN\,m^{-2}}$, which is the standard load value [12], are also monitored.

4. Results of the parametric study

The results of the parametric study of the strengthened reinforced concrete footbridge for different boundary support conditions will be presented in the form of tables. The tables show the deflection u_Q corresponding to the model loaded with the service load. They will also contain the maximum load Q_{max} and the total deflection u_{tot}.

The chapter will be subdivided into sections according to the boundary conditions of the footbridge support into a section for a footbridge fixed at both ends, a footbridge with one hinge support and a footbridge with a hinge at both ends. The tables will then label the different design options A to E according to the list of numerical models in Section 3.2.

4.1. Footbridge fixed at both ends

From the analysis of the footbridge in its ideal state, we obtained information on the critical cross-section of the structure (Figure 6). The results of this design option of the numerical model (A) serve as a reference for the other design options.

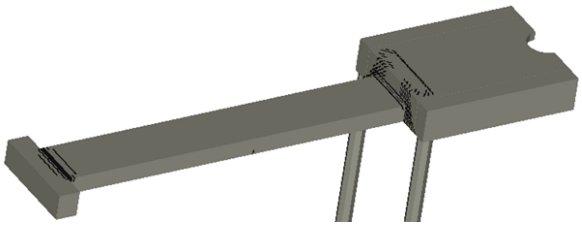

Figure 6. Cracks on the footbridge fixed at both ends, the critical section is at the point where the footbridge is embedded in the tank wall (left support).

Near left support has occured failure for all design options. Strenghtening variants using only shear studs did not have a significant effect on the resulting stiffness of the structure and these variants also show a possible effects of shrinkage. The stiffness was increased only for the variant using shear notches for coupling.

In the case of the evaluation of the maximum load bearing capacity, for the variants considering a degraded structure, a better load bearing capacity can be achieved by any method of coupling.

When comparing the deformations from the applied load, the design option considering shrinkage (C) have higher deformations than the options (D, E) without shrinkage.

By strenghtening the footbridge structure fixed at both ends with a layer of UHPFRC on the upper surface, an increase in the load carrying capacity can be achieved for the degraded structure. The effect of strengthening on the stiffness of the structure for normal service loads depends on the method of coupling and shrinkage of the UHPFRC layer.

4.2. Footbridge with one hinge

From the analysis of the footbridge in the ideal condition with hinge support on one side and fixed support on the other side, we obtained information about the critical cross-section of the structure (Figure 7). The results of this design option of the numerical model (A) serve as a reference for the other design options.

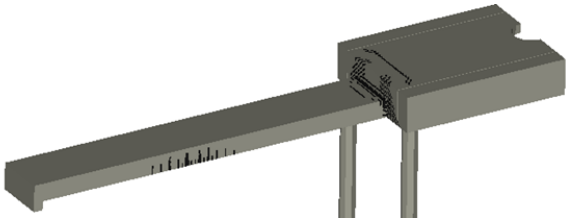

Figure 7. Cracks in a single-hinged footbridge, the critical section is at the centre of the footbridge span.

For all design options, failure occurred in the middle of the span of the footbridge. The conclusions from the analysis of this variant of structure support are almost identical to those for the footbridge fixed at both ends. However, the resulting load bearing capacity of the degraded structure after strengthening does not reach the load bearing capacity of the reference model (design option A).

By strengthening the footbridge with a layer of UHPFRC on the upper surface, an increase in the load-bearing capacity of the degraded structure can be achieved. The effect of strengthening on the stiffness of the structure for normal service loads depends on the method of bonding and shrinkage of the UHPFRC.

4.3. Footbridge with two hinges

From the analysis of the footbridge in its ideal condition with hinged support at both ends, we obtained information about the critical cross-section of the structure (Figure 8). The results of this design option of the numerical model (A) serve as a reference for the other design options.

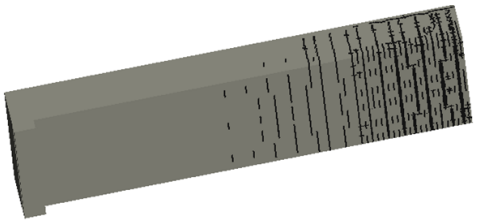

Figure 8. Cracks in a two-hinged footbridge structure (the symmetrical half of the structure was analysed), the critical section is at the centre of the footbridge span.

Design option	u_Q [mm]	Usage [%]	Q_{Max} [kN m^{-2}]	Usage [%]	u_{tot} [mm]
A) Footbridge in ideal state	0.63	100	30	100	18.1
B) Footbridge in degraded state	1.45	230	26	87	48.1
C) Reinforced footbridge. Coupled by studs. with shrinkage	1.93	306	30	100	27.6
D) Reinforced footbridge. Coupled by studs. without shrinkage	1.26	200	30	100	30.3
E) Reinforced footbridge. Coupled by shear nothes and studs	0.73	116	30	100	14.2

Table 3. Evaluation of the deformation and maximum load of the footbridge fixed at both ends.

Design option	u_Q [mm]	Usage [%]	Q_{Max} [kN m^{-2}]	Usage [%]	u_{tot} [mm]
A) Footbridge in ideal state	1.2	100	22	100	36.5
B) Footbridge in degraded state	4.2	350	17	77	34.9
C) Reinforced footbridge. Coupled by studs. with shrinkage	5.13	428	19	86	29.9
D) Reinforced footbridge. Coupled by studs. without shrinkage	3.51	292	19	86	28.1
E) Reinforced footbridge. Coupled by shear nothes and studs	1.86	155	21	95	23.2

Table 4. Evaluation of the deformation and maximum load of the single-hinged footbridge.

Design option	u_Q [mm]	Usage [%]	Q_{Max} [kN m^{-2}]	Usage [%]	u_{tot} [mm]
A) Footbridge in ideal state	11.3	100	10	100	58.9
B) Footbridge in degraded state	46.8	414	6	60	417
C) Reinforced footbridge. Coupled by studs. with shrinkage	10.4	92	11.5	115	598
D) Reinforced footbridge. Coupled by studs. without shrinkage	9.8	87	12.5	125	544
E) Reinforced footbridge. Coupled by shear nothes and studs	7.5	66	13	130	206

Table 5. Evaluation of the deformation and maximum load of the two-hinged footbridge.

For all design options of the two-hinged footbridge analysis, failure occurred in the middle of the footbridge span. For a service load of 5 kN m^{-2}, a reduction in deformation and therefore an increase in the resulting stiffness of the structure was achieved for the design options considering a degraded structure coupled to a UHPFRC slab. Compared to the unstrengthened degraded structure, the resulting values are significantly better.

In the case of the maximum load bearing capacity evaluation, for design options of degraded and strenghtened structure a better load bearing capacity can be achieved by any method of coupling than for the unstrengthened structure in the ideal condition. When comparing the degraded design option with the options considering a strengthening plate, the resulting load bearing capacity is significantly higher.

5. Evaluation of the parametric study

The parametric study was carried out for a total of 15 different design options and offers a range of comparisons. Here, a comparison of the load bearing capacity and the stiffness of the different methods of footbridge supports was made first. Subsequently, the contribution of the strengthening for each degraded design option was evaluated.

A critical point where failure should occur was predicted by analysing the ideal structural condition for each type of footbridge supports. The critical section for the structure fixed at both ends was the section at the tank wall (at the left fixed support). For the single-hinged structure, this was the mid-span of the footbridge. For the footbridge supported by hinges, the critical section is located in the centre of span. The performed analyses confirmed these assumptions. For all design options of each structural system, failure occurred at the predicted location.

The comparison of the stiffness and load bearing capacity of the individual variants of the footbridge supports in the ideal condition was carried out for the maximum achieved load bearing capacity Q_{max} and for the deformation (u_z) from the applied service load (5 kN m^{-2}). The reference is the load bearing capacity of the footbridge fixed at both ends. The results are given in Table 6.

Structural system	Q_{max} [kN m^{-2}]	Usage [%]	u_z [mm]	Usage [%]
Fixed support (both ends)	30	100	0.63	100
Hinged support (one side)	22	73.3	1.2	190.5
Hinged support (both ends)	10	33.3	11.3	1 793

Table 6. Comparison of load bearing capacity and stiffness of the analysed structural systems.

Structural system	Q_{max} [kN m^{-2}]	Usage [%]	u_z [mm]	Usage [%]
B) Footbridge in degraded state	26	100	1.45	100
C) Reinforced footbridge. Coupled by studs. with shrinkage	30	115.4	1.93	133.1
D) Reinforced footbridge. Coupled by studs. without shrinkage	30	115.4	1.26	86.9
E) Reinforced footbridge. Coupled by shear nothes and studs	30	115.4	0.73	50.3

TABLE 7. Comparison of load bearing capacity and stiffness of the footbridge fixed at both ends, 15 % reduction of reinforcement cross-sectional area.

Structural system	Q_{max} [kN m^{-2}]	Usage [%]	u_z [mm]	Usage [%]
B) Footbridge in degraded state	17	100	4.2	100
C) Reinforced footbridge. Coupled by studs. with shrinkage	19	117.6	5.13	122.1
D) Reinforced footbridge. Coupled by studs. without shrinkage	19	117.6	3.51	83.6
E) Reinforced footbridge. Coupled by shear nothes and studs	21	123.5	1.86	44.3

TABLE 8. Comparison of load bearing capacity and stiffness of the single-hinged footbridge, 15 % reduction of reinforcement cross-sectional area.

Structural system	Q_{max} [kN m^{-2}]	Usage [%]	u_z [mm]	Usage [%]
B) Footbridge in degraded state	6	100	46.8	100
C) Reinforced footbridge. Coupled by studs. with shrinkage	11.5	191.7	10.4	22.2
D) Reinforced footbridge. Coupled by studs. without shrinkage	12.5	203.3	9.8	20.9
E) Reinforced footbridge. Coupled by shear nothes and studs	13	216.7	7.47	16.0

TABLE 9. Comparison of load bearing capacity and stiffness of the double-hinged footbridge, 15 % reduction of reinforcement cross-sectional area.

Table 6 shows that, according to theoretical assumptions, the type of support where the footbridge is fixed at both ends achieves the highest load capacity and stiffness. The load bearing capacity of the structure with a hinge on one side is 26.7 % lower and its deformation is 90.5 % higher than for the structure fixed on both sides. The variant with hinges at both ends has clearly the lowest load bearing capacity and stiffness. It has 66.7 % lower load bearing capacity and 1 693 % higher deformation than the footbridge fixed at both ends.

Another comparison will be made for degraded structures with a 15 % reduction of the reinforcement cross-sectional area due to corrosion. The same parameters will be compared as in the case of the comparison of structural systems, i.e. maximum load bearing capacity and deformation from the applied service load. The evaluation is carried out for the footbridge fixed at both ends in Table 7, for the single-hinged footbridge in Table 8 and for the double-hinged footbridge in Table 9. Design options B to E are always compared, where the reference value is the load capacity and stiffness of the unstrengthened structure (option B).

Tables 7–9 show that in all cases the strengthening of the structure increased its load-bearing capacity and in most cases also reduced the deformation of the structure from the applied service load of 5 kN m^{-2}. In all cases, the best results were achieved by the proposed coupling solution in the form of a combination of shear notches with coupling studs (design option E).

For the variants of the footbridge fixed at both ends and the footbridge with one hinge, the increase in load bearing capacity is similar and ranges from 15–24 %. The deformation is higher for the coupled structure than for the un-coupled structure when considering the shrinkage of the UHPFRC slab. Therefore, the shrinkage mainly affects the stiffness of the structure, the load bearing capacity is the same for the variant with and without shrinkage.

The variant with hinged support at both ends has a load bearing capacity for the unstrengthened and degraded structure that is only slightly higher than the comparative load for determining the deformation. Therefore, the unstrengthened variant of the analysis has a significant deflection for this load. The deformation comparison is therefore somewhat biased. In the case that we select the design option in the initial condition for the double-hinged supported structure for comparison (Table 6), we find that there is also an increase in the load bearing capacity and stiffness of the structure for all strengthened degraded structures. Thus, the strengthening effect is most effective for the hinged-supported structure (simple beam).

6. Conclusion

The parametric study was aimed at monitoring the effects of strengthening of existing reinforced concrete footbridge with a 50 mm thick UHPFRC slab on the upper surface. It investigated the effect of different parameters affecting the stiffness and load bearing capacity of the footbridge (different methods of supporting of the footbridge, the effect of concrete degradation and reinforcement corrosion, the method of coupling of reinforced concrete and UHPFRC and the effect of shrinkage of the strengthening slab). An analysis of the ideal state of the structure without strengthening and concrete or reinforcement degradation was carried out for each support option. This was followed by an analysis for structures with degraded concrete (lower modulus of elasticity, tensile and compressive strength) and with a 15 % reduction in reinforcement cross-sectional area due to corrosion. The structures with degradation were then strengthened with UHPFRC slab. The structure was coupled either with coupling studs only or with a combination of studs and shear notches.

The results of the parametric study show that the effect of the UHPFRC strengthening layer on the top surface has a different positive effect on the behaviour of the structure for different support types. The most pronounced benefit of the strengthening is for a structure with hinges at both ends, where the strengthening layer is located in the compression region of the cross-section and the excellent compressive properties of the UHPFRC can be exploited to the maximum.

When designing the strengthening, it is necessary to take into account the possible effect of shrinkage of the UHPFRC strengthening layer and to select the optimum coupling method. Although the use of a combination of shear notches with coupling studs leads to a significantly higher overall stiffness of the final composite structure, it is much more challenging to implement.

Acknowledgements

This article was published with the support of the grant project OP TAK CZ.01.01.01/01/22_002/0000725 Strengthening and renovation of industrial buildings using UHPC material.

References

[1] M. K. Ismail, A. A. Hassan. Structural performance of large-scale concrete beams reinforced with cementitious composite containing different fibers. *Structures* **31**:1207–1215, 2021. https://doi.org/10.1016/j.istruc.2021.02.028

[2] M. Qiu, J. Cao, Z. Shao, et al. Flexural cracking behavior of steel-NC-UHPC composite beam under negative bending moment. *Engineering Structures* **322**:119071, 2025. https://doi.org/10.1016/j.engstruct.2024.119071

[3] N. Bertola, P. Schiltz, E. Denarié, E. Brühwiler. A review of the use of UHPFRC in bridge rehabilitation and new construction in switzerland. *Frontiers in Built Environment* **7**:769686, 2021. https://doi.org/10.3389/fbuil.2021.769686

[4] J. Abellán-García, J. S. Carvajal-Muñoz, C. Ramírez-Munévar. Application of ultra-high-performance concrete as bridge pavement overlays: Literature review and case studies. *Construction and Building Materials* **410**:134221, 2024. https://doi.org/10.1016/j.conbuildmat.2023.134221

[5] Z. Haber, I. De La Varga, J. F. Munoz, B. A. Graybeal. UHPC overlays for highway bridge decks: Bond behavior, durability, and structural performance. In *Second International Interactive Symposium on UHPC*. Iowa State University Digital Press, 2019. https://doi.org/10.21838/uhpc.9719

[6] W. Nadir, M. M. Kadhim, A. Jawdhari, et al. Experimental investigation on UHPC-NSC composite beams. *Structures* **60**:105885, 2024. https://doi.org/10.1016/j.istruc.2024.105885

[7] M. Holy, D. Citek, P. Tej, V. Lukáš. Flexural strength of thin slabs made of UHPFRC. *Solid State Phenomena* **292**:224–229, 2019. https://doi.org/10.4028/www.scientific.net/SSP.292.224

[8] S. He, X. Huang, H. Zhong, et al. Experimental study on bond performance of UHPC-to-NC interfaces: Constitutive model and size effect. *Engineering Structures* **317**:118681, 2024. https://doi.org/10.1016/j.engstruct.2024.118681

[9] S. He, X. Huang, J. Huang, et al. Shear bond performance of UHPC-to-NC interfaces with varying sizes: Experimental and numerical evaluations. *Buildings* **14**(11):3684, 2024. https://doi.org/10.3390/buildings14113684

[10] A. M. Jabbar, A. S. Al-Zuheriy, Q. A. Hasan. A numerical investigation of the structural behavior of reinforced concrete beams fully or partially encased with UHPC layers in flexure. *Structures* **70**:107706, 2024. https://doi.org/10.1016/j.istruc.2024.107706

[11] V. Červenka, L. Jendele, J. Červenka. ATENA program documentation. Part 1: Theory. [2025-01-29]. https://www.technologismiki.com/uplx/ATENA_Theory.pdf

[12] Eurocode1 : Actions on structures. Standard, The National Annex, Prague, 2005.